Thermal Elasto-Plastic Analysis on Stress and Strain in Weld Metal during Multi-pass Welding†

Kunihiko SATOH*, Kenji SEO, Kenji IWAI*** and Daisuke TAKAHASHI******

Abstract

This paper is concerned with the elasto-plastic analysis of thermal stresses and strains in weld metal of multi-pass butt welding. An analysis is performed based on the incremental theory under one dimensionally distributed temperature. Numerical calculations are made for two kinds of weld joint as shown in Figs. 1 (b), (c), each of which corresponds to the behavior of the transverse and longitudinal direction of weld joint respectively. It is assumed that a rectangular distribution of initial temperature is given at the start of each pass and heat flow occurs only in y-direction. Another assumption applied to the calculations is that a line heat source is given at the start of each pass and two dimensional heat flow occurs.

From the calculations are estimated transient thermal stress and plastic strain distributions. The effects of weld conditions on residual stress and strain are clarified. The relations between plastic strain on the back surface of the first pass and angular distortion under several weld conditions are also obtained.

1. Introduction

Most of the studies on thermal stress and strain during welding are dealt with macroscopic distributions of stress and strain in a weldment.[1] There remain many unknown factors on local stress and strain produced in the weld metal and its vicinity, which are of vital importance in relation to such a phenomenon as weld crack. Particularly, it can be said that no analytical study on local stress and strain produced in the weld metal during multi-pass welding has been carried out.

In this paper, thermal elasto-plastic analysis is performed to obtain fundamental knowledge concerned with local stress and strain produced in weld metal during multi-pass welding. Recently, finite element method has come into use as one of the methods of numerical calculation for thermal elasto-plastic analysis.[2), 3)]

Although this method has the possibility to apply it to general cases of thermal stress and strain problems, it has the following disadvantages; 1) excessive calculating time is required for analysis and 2) parametric arrangement is difficult.

In this study calculation is made by using one dimensional thermal elasto-plastic analysis based on the incremental theory.[4)]

2. Theory

2.1 Model for multi-pass butt welding

The welding stress and strain produced in the weld metal of multi-pass weld joint as shown in **Fig. 1 (a)** is discussed. An analysis is performed based on the assumption that weld metal having initial temperature To is instanteneously superimposed one after another by throat depth a. Numerical calculations are made for two kinds of model; axial force and bending moment are zero in a model as shown in **Fig. 1 (b)** and curvature is zero in a model as shown in **Fig. 1 (c)** at any instance of thermal cycles. Each of the models corresponds to the behavior of the transverse and longitudinal direction of weld joint respectively.

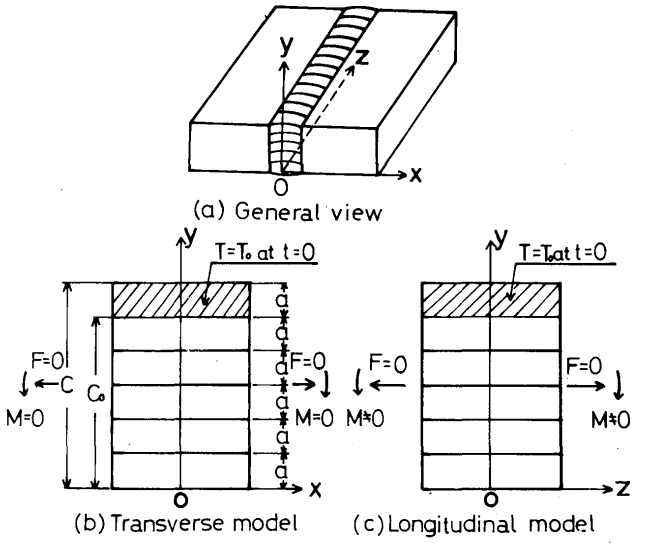

Fig. 1. Two kinds of model corresponded to the behavior of the transverse and longitudinal direction of multi-pass weld joint.

† Received on July 18, 1973 (I.I.W. Doc. X—706—73)

* Professor

** Research Associate, Dept. of Welding Engineering, Faculty of Engineering, Osaka University

*** Graduate student, Osaka University

**** Co-operative Researcher (1973), Nippon Steel Corporation

2.2 Temperature distribution

When the throat depth becomes C after being superimposed the weld metal having initial temperature T_0 as shown in **Fig. 1 (b),** temperature distribution T (y, t) at a given time t can be obtained by Eq. (1). This equation is given based on the assumption that the heat transfers only to the y direction and reflects from the back surface (y=0).

$$\mathbf{T}(y,t)=\frac{\mathbf{T}_0}{2}\sum_{n=1}^{\infty}\left[\phi\left(\frac{2(n-1)c-y+c+a}{2\sqrt{kt}}\right)-\phi\left(\frac{2(n-1)c-y+c-a}{2\sqrt{kt}}\right)\right]+\frac{\mathbf{T}_0}{2}\sum_{n=1}^{\infty}\left[\phi\left(\frac{2nc+y-c+a}{2\sqrt{kt}}\right)-\phi\left(\frac{2nc+y-c-a}{2\sqrt{kt}}\right)\right] \quad (1)$$

where $\phi(z)=\frac{2}{\sqrt{\pi}}\int_0^z e^{-u^2}du$

k: thermal diffusivity

The following dimensionless variables being introduced,

$$\left.\begin{aligned}&\tau=\alpha\mathbf{T}/\varepsilon_{\mathbf{Y}_0},\quad \tau_0=\alpha\mathbf{T}_0/\varepsilon_{\mathbf{Y}_0},\quad \eta=y/c\\&\eta_0=a/c,\quad \kappa=2\sqrt{kt}/c\end{aligned}\right\} \quad (2)$$

where **E:** Young's modulus α: Linear expansion coefficient
$\sigma_{\mathbf{Y}_0}$: Yield strength of material at reference temperature

$\varepsilon_{\mathbf{Y}_0}=\sigma_{\mathbf{Y}_0}/\mathbf{E}$

Eq. (1) can be re-expressed as Eq. (3).

$$\tau(\eta,\kappa)=\frac{\tau_0}{2}\sum_{n=1}^{\infty}\left[\phi\left(\frac{2(n-1)-\eta+1+\eta_0}{\kappa}\right)-\phi\left(\frac{2(n-1)-\eta+1-\eta_0}{\kappa}\right)\right]+\frac{\tau_0}{2}\sum_{n=1}^{\infty}\left[\phi\left(\frac{2n+\eta-1+\eta_0}{\kappa}\right)-\phi\left(\frac{2n+\eta-1-\eta_0}{\kappa}\right)\right] \quad (3)$$

Numerical calculation of the temperature distribution is repeated until the value in the brackets becomes less than 1.0×10^{-7}. The temperature is cooled to 0°C after the temperature distribution has come almost even (difference of temperature between the front and back surface is less than 1°C).

2.3 Thermal elasto-plastic analysis

Incremental theory by I. Tsuji[4] is applied to the thermal elasto-plastic analysis. The variables used are shown in **Table 1.**

Table 1. Variables used.

Item		Mark	Nondimension
Time		t	$\kappa=2\sqrt{kt}/C$
Location		y	$\eta=y/C$
Stress		σ	$s=\sigma/\sigma_{Y_0}$
Yield strain		ε_Y	$e_Y=\sigma_Y/E$
Strain		ε	$e=\varepsilon/\varepsilon_{Y_0}$
Plastic strain		ε_P	$e_P=\varepsilon_P/\varepsilon_{Y_0}$
Temperature		T	$\tau=\alpha T/\varepsilon_{Y_0}$
Moment		M^*	$M=M^*/C^2\sigma_{Y_0}$
Material constant	Thermal diffusivity	k	—
	Young's modulus	E	—
	Thermal expansion	α	—
	Yield strength dependent on temperature	q	$n=q\varepsilon_{Y_0}/\alpha$
	Strain hardening	h	$m=h\varepsilon_{Y_0}$
	Yield strength	σ_Y	$s_Y=\sigma_Y/\sigma_{Y_0}$

Temperature dependency and strain hardening dependency of yield strength of the material are assumed as Eq. (4).

$$\left.\begin{aligned}&\mathbf{T}\le\frac{1}{q},\quad \sigma_{\mathbf{Y}}=\sigma_{\mathbf{Y}_0}(1-q\mathbf{T})(1+h\bar{\varepsilon}_p)\\&\mathbf{T}>\frac{1}{q},\quad \sigma_{\mathbf{Y}}=0\end{aligned}\right\} \quad (4)$$

where q: Material constant for temperature dependency of yield strength
h: Material constant for strain hardening dependency of yield strength

$\bar{\varepsilon}_p=\Sigma\left|\Delta\varepsilon_p\right|$

$\Delta\varepsilon_p$: Plastic strain increment

Dimensionless expression of Eq. (4) is given as Eq. (5).

$$\left.\begin{aligned}&\tau\le 1/n,\quad s_Y=e_Y=(1-n\tau)(1+m\bar{e}_p)\\&\tau>1/n,\quad s_Y=e_Y=0\end{aligned}\right\} \quad (5)$$

where $\bar{e}_p=\Sigma\left|\Delta e_p\right|$, $\Delta e_p=\Delta\varepsilon_p/\varepsilon_{Y_0}$

Also, strain increment for the time period $\Delta\kappa$ from κ_i to κ_{i+1} can be obtained from Eq. (6) at a point η distant from the back surface under constrained conditions, that is, free circumference (axial force and bending moment are zero) and curvature zero as shown in **Fig. 1 (b), (c).**

$$\left.\begin{aligned}&\Delta e=\Delta a+\Delta b\cdot\eta-\Delta\tau \quad \text{(free circumference)}\\&\Delta e=\Delta a-\Delta\tau \quad \text{(curvature is zero)}\end{aligned}\right\} \quad (6)$$

where

$$\Delta a = \frac{-L_{3E}\cdot\Delta P + L_{2E}\cdot\Delta Q}{L_{2E}^2 - L_E\cdot L_{3E}},$$

$$\Delta b = \frac{L_{2E}\cdot\Delta P - L_E\cdot\Delta Q}{L_{2E}^2 - L_E\cdot L_{3E}}$$

curvature $B = \Sigma\Delta b$ (free circumference)

$$\Delta a = \frac{\Delta P}{L_E} \quad \text{(curvature is zero)}$$

$$\Delta P = \int_0^1 g\Delta\tau d\eta - \int_0^1 (1-g)(\mathrm{sgn}\ \Delta e_Y)\, d\eta$$

$$\Delta Q = \int_0^1 g\Delta\tau\eta d\eta - \int_0^1 (1-g)(\mathrm{sgn}\ \Delta e)\,\eta d\eta$$

$$L_E = \int_0^1 g d\eta,\quad L_{2E} = \int_0^1 g\eta d\eta,\quad L_{3E} = \int_0^1 g\eta^2 d\eta$$

$$g = \begin{cases} 1 \text{...elastic zone} \\ 0 \text{...plastic zone} \end{cases} \qquad \mathrm{sgn} = \begin{cases} +1 \text{...Tensile stress} \\ -1 \text{...Compressive stress} \end{cases}$$

$\Delta\tau$: Temperature increment during the time period from κ_i to κ_{i+1}

From Eq. (5), increment of yield strength becomes

$$\Delta s_Y = \Delta e_Y = m(1-n\tau_i)\left|\Delta e_p\right| - n(1+m\bar{e}_i)\Delta\tau \quad \text{..... (7)}$$

The equation (8) gives the yield conditions.

$$\left.\begin{array}{l} \text{If } s_i^2 < \{(1-n\tau_i)(1+m\bar{e}_i)\}^2 \text{ or} \\ \quad \Delta e \pm (1+m\bar{e}_i)\, n\Delta\tau \lessgtr 0 \text{ and } s_i = \pm\{(1-n\tau_i)(1+m\bar{e}_i)\} \end{array}\right\} \begin{array}{l} \Delta e_p = 0 \\ g = 1 \end{array}$$

$$\text{If } \Delta e \pm (1+m\bar{e}_i)\, n\Delta\tau \gtrless 0 \text{ and } s_i = \pm\{(1-n\tau_i)(1+m\bar{e}_i)\}$$

$$\Delta e_p = \frac{\Delta e \pm (1+m\bar{e}_i)\, n\Delta\tau}{1+m(1-n\tau_i)},\quad g = 0$$

.....(8)

When Δe and Δe_p at each point are calculated, stress increment can be obtained from Eq. (9).

$$\Delta s = \Delta c - (1-g)\,\Delta e_p \quad \text{..... (9)}$$

s_i, τ_i and $\bar{e}_i$ in Eqs. (6), (7) and (8) represent stress, temperature and plastic strain, respectively.

In the numerical calculation, the following values are adopted.

Temperature dependency of yield strength (see **Fig. 2**):

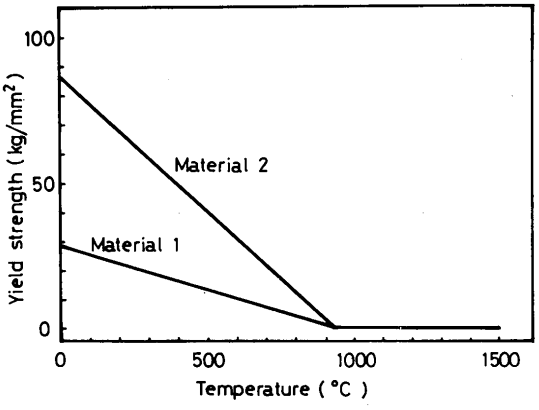

Fig. 2. Yield strength of the materials used for analysis.

Material 1 $\sigma_{Y_0}\cdot q = \dfrac{28.7}{930}$ (i. e. n=0.1)

Material 2 $\sigma_{Y_0}\cdot q = \dfrac{86.1}{930}$ (i. e. n=0.3)

Strain hardening dependency of yield strength:

h=10 (i. e. m=0.0137)

Linear expansion coefficient:

$\alpha = 1.47\times10^{-5}\,°C^{-1}$

Initial temperature of weld metal:

$T_0 = 1500°C$ (i. e. $\tau_0 = 16.0$)

The relationship between initial temperature and weld heat input will be studied later in Paragraph 3.4.

3. Transient thermal stress and plastic strain

3.1 Stress and plastic strain distribution

It has been assumed that stress and strain after the first pass weld are not produced because of the uniform contraction of weld metal. Transient stress and plastic strain after the second pass weld are described in this paragraph.

Curve B in **Fig. 3** shows the transient curvature in the transverse direction (x direction) to the weld line. In the early stage, convex deformation on the front surface is observed and then reverse deformation is produced as the heat transfers to the back. And this deformation continues untill temperature at the section becomes even. The time κ after welding required for the temperature to become even within

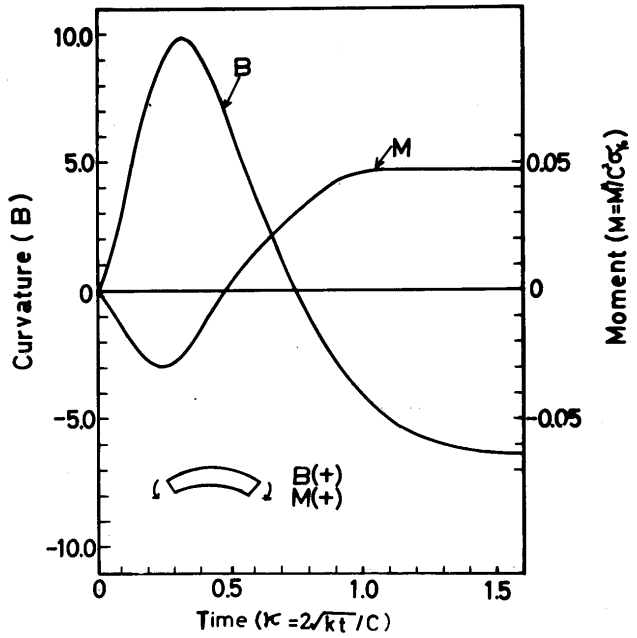

Fig. 3. Transient curvature in the transverse direction and bending moment in the longitudinal direction after the second pass weld.

2 % or 0.5 % difference is 1.50 or 1.85, respectively. Bending moment is produced in the section along the longitudinal direction of the weld line (z direction) as indicated by curve M in **Fig. 3.**

Figure 4 shows transient thermal stress distributions produced in the transverse and longitudinal direction. The abscissa indicates a distance from the back surface of the first pass.

At the early stage (for example, the time after the second pass weld, $\kappa=0.029$), the stresses which appear in the transverse direction are as follows; tensile stress in the weld metal of the second pass, compressive stress with a high value in the vicinity of the front surface of the first pass, tensile stress in the middle of the first pass and compressive stress on the back surface of the first pass. As time passes, stresses at each location, however, reverse and finally the residual stresses become compressive on the front surface of the second pass, tensile in the middle and the back surface of the second pass and the front surface of the first pass, compressive in the middle and tensile on the back surface of the first pass.

At the early stage (for example, $\kappa=0.032$), the stresses which appear in the longitudinal direction are as follows; tensile stress in the second pass, compressive stress in the vicinity of the front surface of the first pass and tensile stress in the middle and the back surface of the second pass. As time passes ($\kappa=0.378$), stress distribution changes as follows; tensile stress in the second pass and the vicinity of the front surface of the first pass, compressive stress in the middle of the first pass and tensile stress on the back surface of the first pass. And finally the residual stresses become tensile in the second pass and compressive in the first pass. The reason why the values of residual stresses in **Fig. 4** are considerably small compared with the yield strength at the reference temperature is because the average temperature in the section becomes high.

Figure 5 shows transient plastic strain distributions.

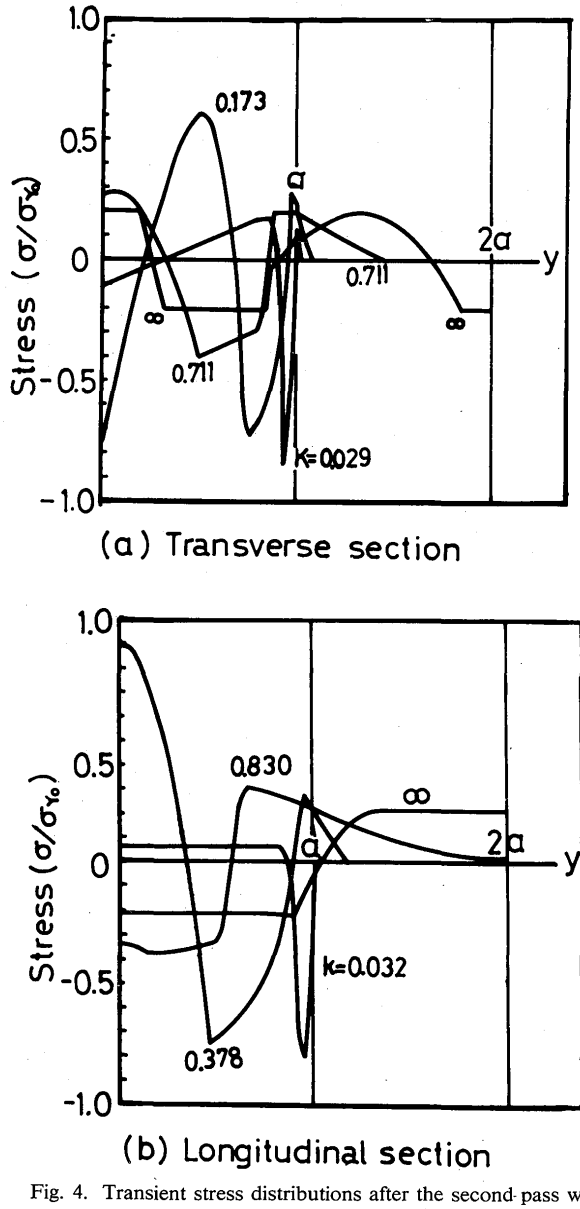

Fig. 4. Transient stress distributions after the second pass weld.

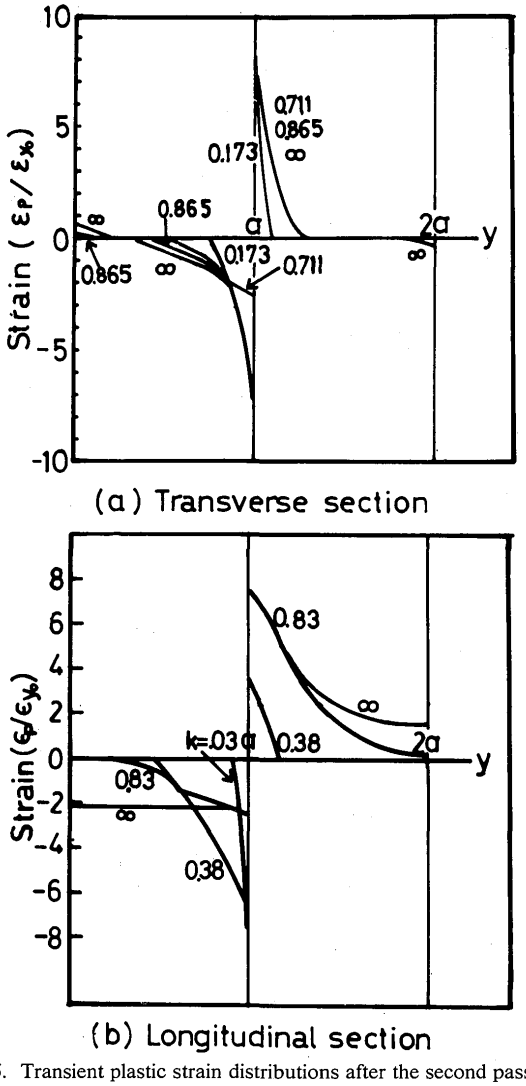

Fig. 5. Transient plastic strain distributions after the second pass weld.

(In this paper, plastic strain is defined as the algebraic sum of plastic strain received at the temperature less than 930°C) Plastic strain of compression on the front surface of the second and first passes and that of tension on the back surface of the second and first passes are produced in the transverse direction. Tensile plastic strain in the second pass and compressive plastic strain in the first pass are produced in the longitudinal direction.

3.2 Effect of residual stress by second pass weld

Figure 6 shows transient stresses after the third pass weld carried out when residual stress and plastic strain produced by the second pass weld still remain. **Figure 7** shows transient plastic strain distributions. In this case, distributions of transient stress are considerably complex due to the existence of residual stress (indicated with the broken line in **Fig. 6**) by the second pass weld. It is redistributed as time passes and finally residual stress distribution becomes curve $\kappa=\infty$ in **Fig. 6.** Provided that no residual stress is produced by the second pass weld, distribution of residual stress after the third pass weld is indicated by one dotted chain line in **Fig. 6.** Comparing these two curves, existence of residual stress by the second pass weld has little influence on residual stress distribution after the third pass weld.

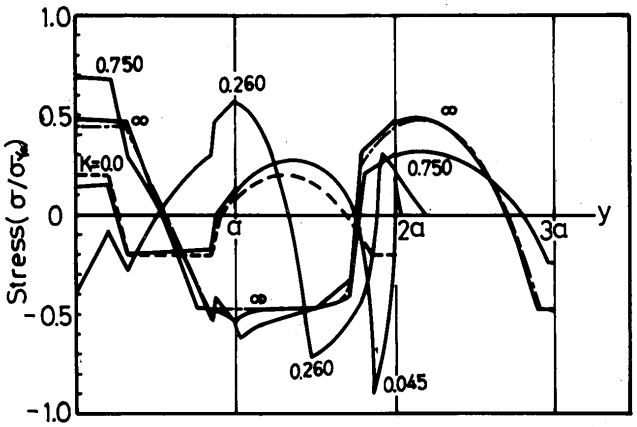

(a) Transverse section

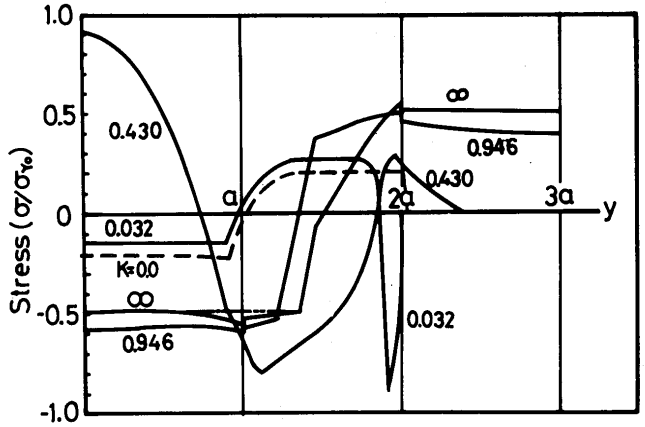

(b) Longitudinal section

Fig. 6. Transient stress distributions after the third pass weld.

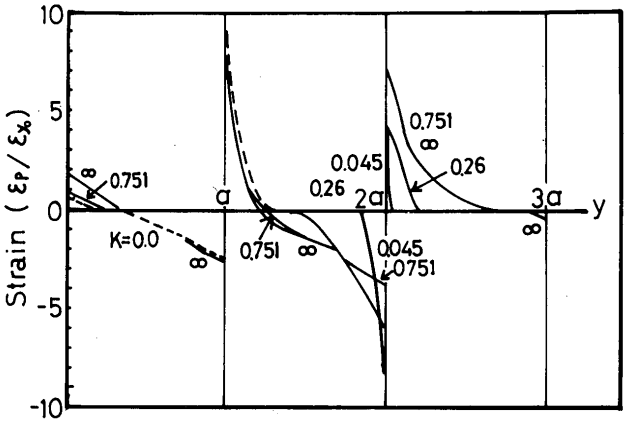

(a) Transverse section

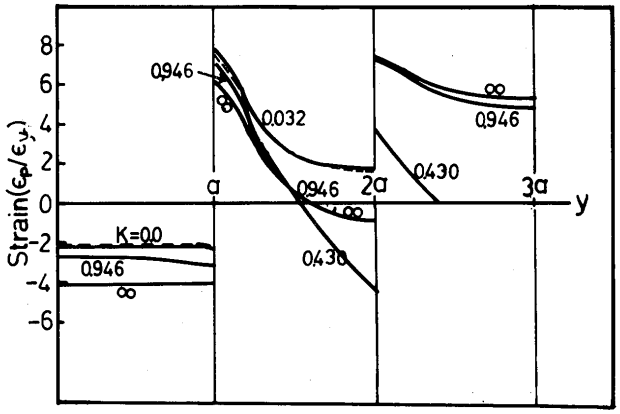

(b) Longitudinal section

Fig. 7. Transient plastic strain distributions after the third pass weld.

3.3 Transient thermal stress as time passes

Figure 8 shows transient stress in several positions. **Figure 8 (a)** indicates the stress in the transverse direction and **Fig. 8 (b)** that in the longitudinal direction.

Stress at the back surface of the first pass is compressive in the early stage as indicated by curve 1, but it changes into tensile as time passes, reaches the maximum at $\kappa \fallingdotseq 0.8$ and finally becomes the value corresponding to the yield strength of the average temperature. In the early stage, compressive stress on the front surface of the first pass and tensile stress on the back surface of the second pass are produced and as time passes both become almost equal value, which are indicated by curves 2 and 3. Stress on the front surface of the second pass keeps 0 until $\kappa \fallingdotseq$ 0.85 because of high temperature, but compressive

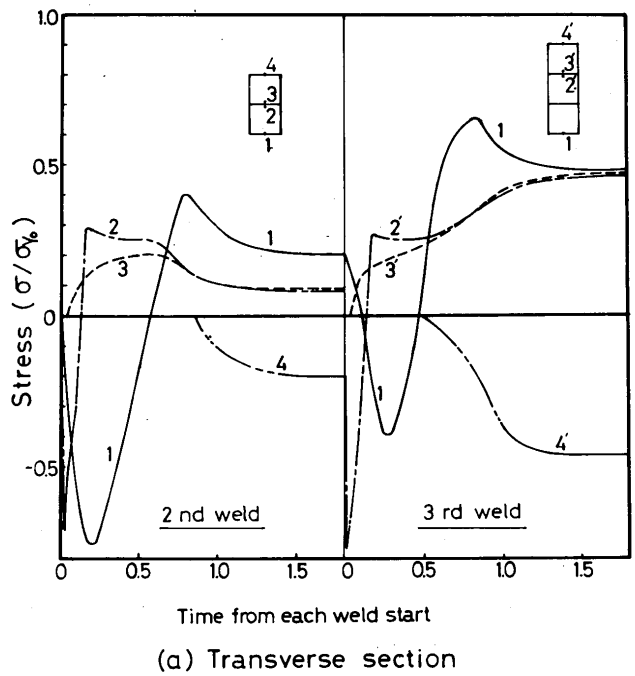

(a) Transverse section

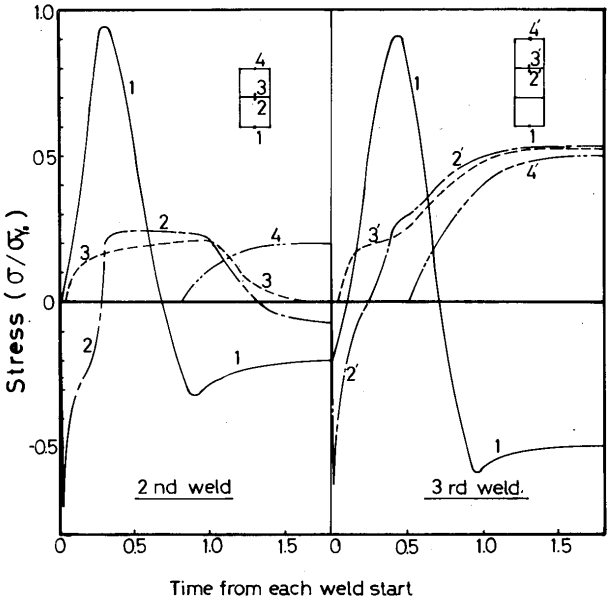

(b) Longitudinal section

Fig. 8. Transient thermal stress in several positions as time passes.

stress is produced as the temperature becomes lower, as indicated by curve 4 and the stress corresponding to the yield strength of the average temperature finally remains.

Transient stress after the third pass weld as shown in the right half of **Fig. 8 (a)** has the similar tendency to that in the case of the second pass weld.

Figure 8 (b) indicates transient stress in the longitudinal direction, in which case compressive stress on the front surface of the second pass and tensile stress on the back surface of the first pass are contrary to those in the transverse direction because bending deformation is constrained. At the boundary of each pass, however, the similar tendency of stress to that in the transverse direction is observed because of little effect of bending moment.

3.4 Consideration on initial temperature of weld metal

In the preceding paragraphs, the heat input given is only 6300 joule/cm, if both depth and width of each pass are 10 mm. This heat input is considerably smaller than that given at the actual welding and can not correspond to that of the actual welding. This is due to the fact that heat in the actual welding transfers two-dimensionally. In this paragraph the calculation result is described when the heat transfers two-dimensionally.

When the weld metal of the nth pass is placed as shown in **Fig. 9,** thermal elasto-plastic analysis is done assuming that heat source Q joule/cm is given momentarily on the surface of the weld metal of the nth pass and the temperature on y-axis distributes uniformly towards the x direction. Temperature distribution at the moment when the temperature at the back surface of the nth pass (point η_n in **Fig. 9**) rises to melting temperature (1500°C), is used as the initial condition. The throat depth a of each weld pass is determined in order that the maximum temperature at the point of the back surface of the nth pass becomes exactly 1500°C, by which is established law of similarity that does not require individual calculation for any change of heat input. For example, when heat input is 21,000 joule/cm, throat depth is decided as 0.88 cm.

The temperature becomes uniform at approximately 650°C after the second pass weld by using the same way for the heat transfer. Conversing this to the initial temperature of rectangular heat source described in Paragraph 2, it becomes 1300°C and thereby it is proved that temperature 1500°C is slightly excessive as To.

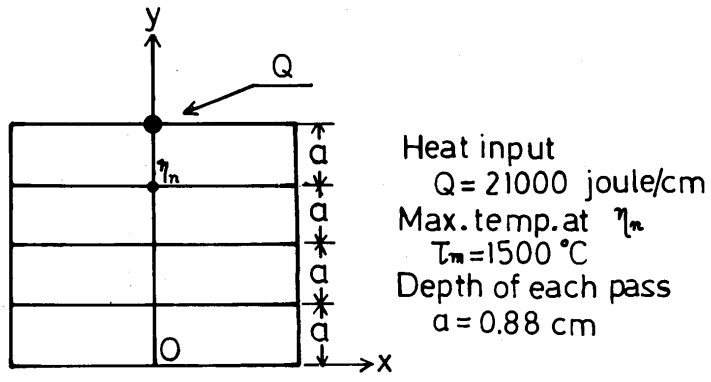

Fig. 9. A model in case that a line heat source is given at the start of each pass.

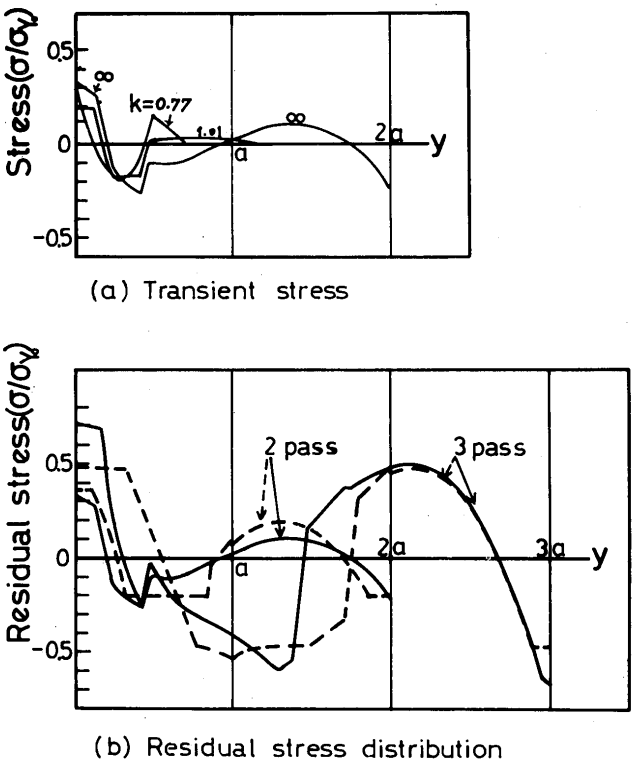

Fig. 10. Transient and residual stress distributions in the case of a line heat source.

Figure 10 (a) indicates transient stress in the transverse direction when the second pass is superimposed. In early stage, distributions of stress in **Fig. 10 (a)** differ from those shown in **Fig. 4 (a),** but distribution of residual stress is similar to that, which fact can be more clearly understood by observing distributions of residual stress after the second and third pass welds. In **Fig. 10 (b),** the full lines show distributions of residual stress in the case of two-dimensional heat transfer, the broken lines the results of analysis by one-dimensional heat transfer as shown in **Fig. 4 (a)** and **Fig. 6 (a).** Both have almost the same distributions of stress.

4. Effects of welding conditions on residual stress and plastic strain

4.1 Weld pass

Figure 11 shows each distribution of residual stress which appears after the second to the sixth pass welding. **Figure 11 (a)** indicates distributions of stress in the transverse direction (x direction) and (b) those in the longitudinal direction (z direction). **Figure 11 (a)** shows that when the temperature distribution becomes even, the back surface of the first pass is yielded in every pass and tensile residual stress at this point corresponds to the yield strength of the

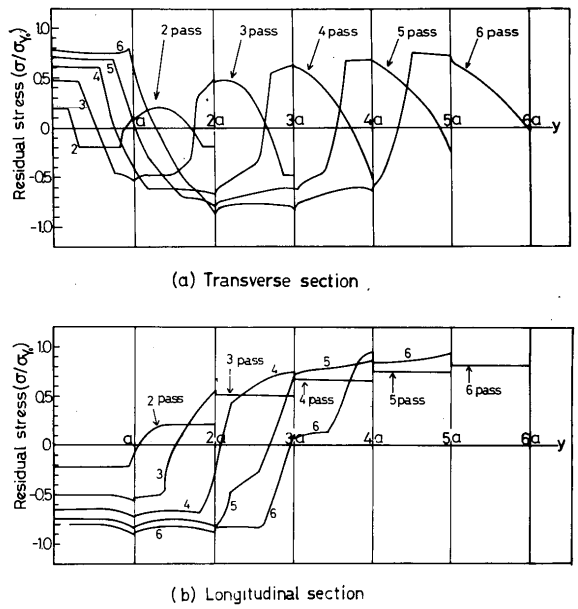

Fig. 11. Residual stress distributions in multi-pass welding.

average temperature. On the front surface of the last pass, compressive residual stress exists due to bending deformation in the case of the small number of passes. Bending deformation tends to become smaller as the number of passes increases and stress on the surface of the last pass transfers towards the tensile side. This is because bending rigidity becomes larger as the number of passes increases and as a result it is difficult to produce bending deformation. A high tensile residual stress exists at the front surface of the pass just below the last pass in any case after the third pass. This tensile residual stress may be one of the dynamical factors for reheating crack observed in multi-pass welding of HY 80 steel by Kobayashi and others.[6] Residual stress in the longitudinal direction indicated in (b) is compressive at the back side and tensile at the front side. A considerably high tensile residual stress exists at the front surface of the pass just below the last pass as the number of passes increases, as in the case of **Fig. 11 (a).** This may be considered as one of the causes to transverse crack[7] produced by multi-pass submerged arc welding.

The full line in **Fig. 12** shows distributions of

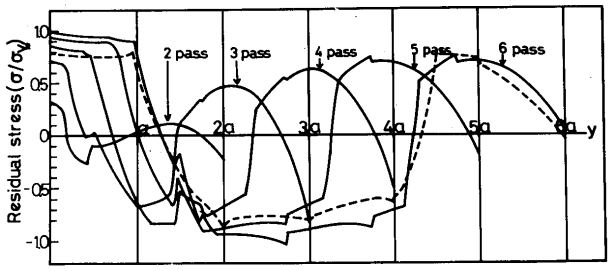

Fig. 12. Residual stress distributions in the case of a line heat source.

residual stress in the transverse direction in case temperature distribution is given by two-dimensional heat transfer as described in Paragraph 3.4. The broken line in **Fig. 12** shows the distribution of residual stress after sixth pass weld as shown in **Fig. 11 (a).** Both lines show remarkable similarity.

Figure 13 shows each distribution of residual plastic strain which appers after the second to sixth pass welding. **Figure 13 (a)** indicates the distributions of plastic strain in the transverse direction (x direction) and (b) in the longitudinal direction (z direction). **Figure 13 (a)** shows that a high tensile plastic strain on the back surface of each pass occurs. Almost linear relationship between plastic strain on the back surface of the first pass and the number of passes is observed as shown in **Fig. 14.** On the other hand, **Fig. 13 (b)** shows that compressive plastic strain at the first pass and tensile plastic strain at the last pass remain.

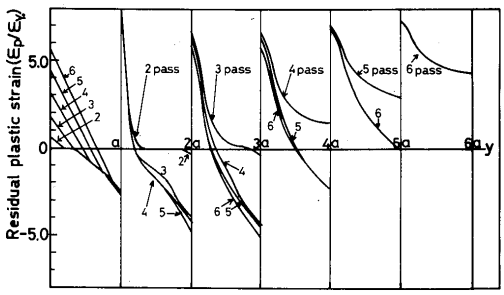

(a) Transverse section

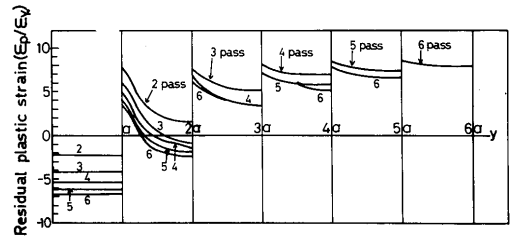

(b) Longitudinal section

Fig. 13. Residual plastic strain distributions in multi-pass welding.

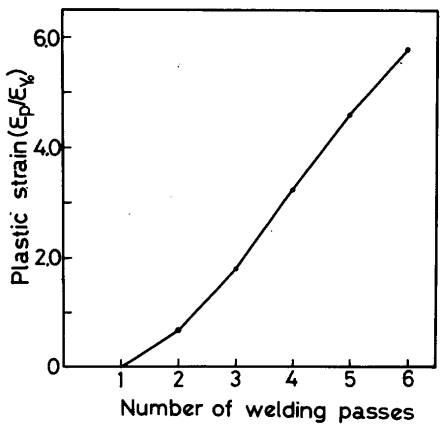

Fig. 14. Relationship between plastic strain on the back surface of the first pass and the number of weld passes.

4.2 Heat input

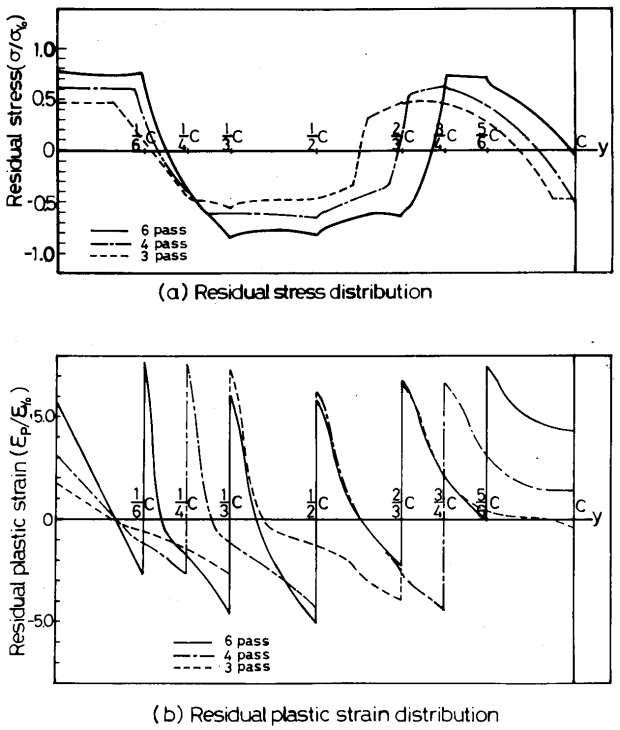

(a) Residual stress distribution

(b) Residual plastic strain distribution

Fig. 15. Effect of heat input on residual stresses and plastic strains.

Figure 15 shows the distributions of residual stress and plastic strain in the transverse direction, when welding for the same throat depth C is completed by three, four or six passes of weld respectively. When welding is completed by the small numbers of weld pass (large heat input), residual stress becomes small and plastic strain on the back surface of the first pass also becomes small. According to the results of Cranfield type cranking test by Araki and others[8], it is reported that crack from the root by four passes of MIG welding has smaller cracking percentage than that by seven passes of shield metal arc welding and three passes of submerged arc welding further lowers the cracking percentage. This fact is mainly due to difference of diffusive hydrogen or welding method. However, a large heat input welding shows effectiveness for crack at the point of view of stress and strain.

4.3 Interpass temperature

The effect of interpass temperature on thermal stress and plastic strain in multi-pass welding is studied. Analysis is made under the condition that interpass temperature is approximately 150°C.

Figure 16 indicates how residual stress and plastic strain both on the front surface of the last pass and on the back surface of the first pass change with the increase of weld passes. Full lines in **Fig. 16** show

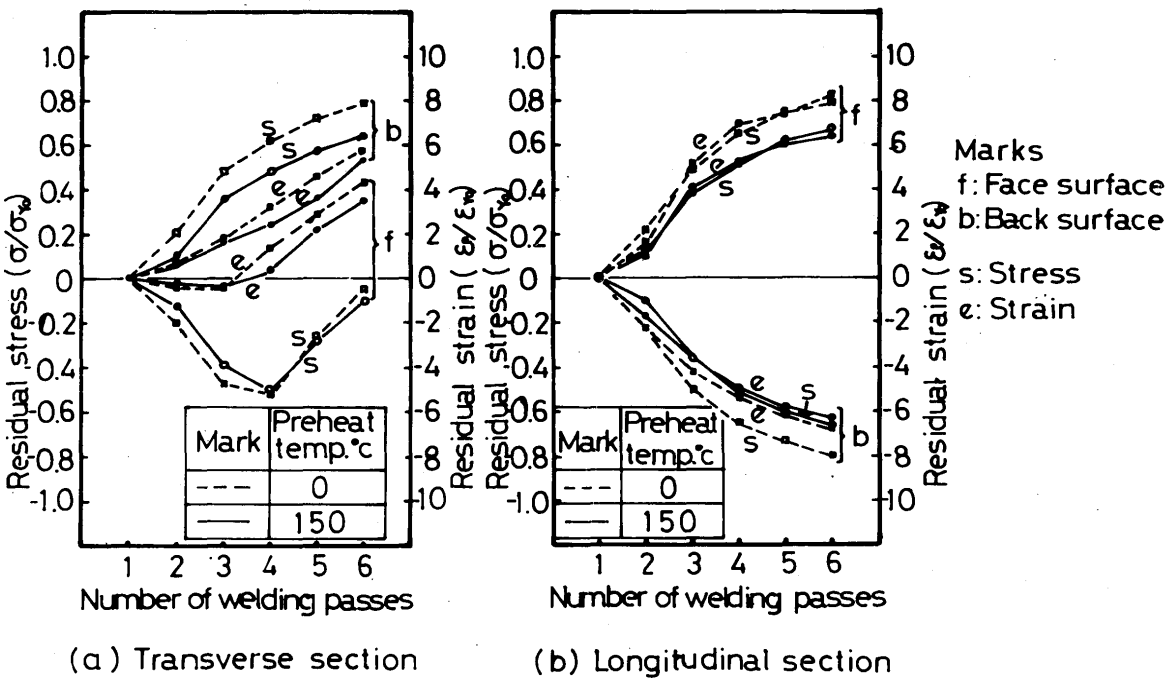

Fig. 16. Effects of interpass temperature on residual stresses and plastic strains.

the residual stress and plastic strain at interpass temperature 150°C and broken lines show those at 0°C. It indicates that residual stress and plastic strain become smaller as interpass temperature becomes higher. It is well-known fact that preheat is one of the effective means to prevent weld crack from the view of diffusing hydrogen out of weld and softening the hardened structure. It is considered that preheat is also effective for reduction of residual stress and plastic strain.

4.4 Yield strength of weld metal

Yield strength of weld metal used in the preceding paragraph is 28.7 kg/mm^2 (Material 1 in **Fig. 2**) and the result of analysis by using weld metal having yield strength 86. 1 kg/mm^2 (Material 2) is described in the following.

Figure 17 indicates how residual stress and plastic

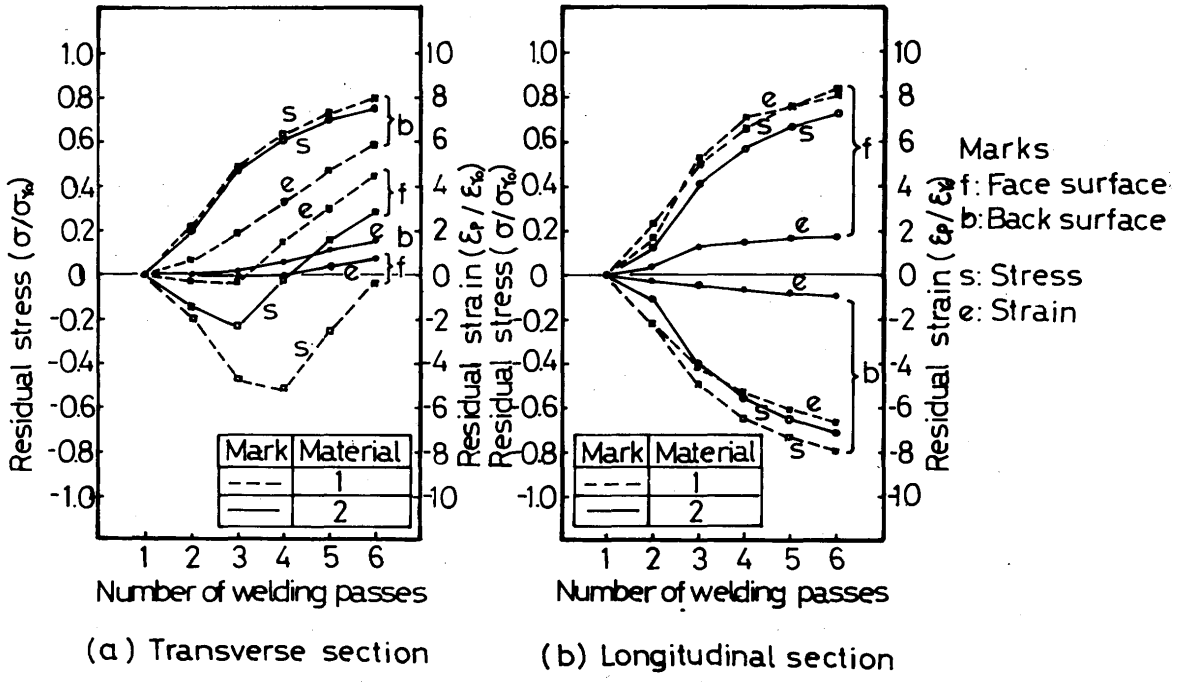

Fig. 17. Effects of yield strength of weld metal on residual stresses and plastic strains.

strain on the front surface of the last pass and the back surface of the first pass change with the increase of weld passes. Broken lines in **Fig. 17** show the residual stress and plastic strain in the case of yield strength 28.7 kg/mm^2. The ordinate in **Fig. 17** indicates non-dimensional values of stress for yield strength of each weld metal. **Figure 17 (a)** proves that residual stress on the back surface of the first pass is little affected by the yield strength of weld metal. Because the residual stress on the back surface of the first pass corresponds to the yield strength of the average temperature as described in Paragraph 4.1. Plastic strain, however, becomes remarkably small when yield strength is high. On the other hand residual stress on the front surface of the last pass in the case of yield strength 86.1 kg/mm^2 is more tensile than that in the case of yield strength 28.7 kg/mm^2, because angular distortion is small when yield strength is higher.

In the case of **Fig. 17 (b),** residual stress shows little change, because stress corresponding to the yield strength of the average temperature remains both on the front and back surfaces. Plastic strain, however, becomes remarkably small when yield strength is high.

5. Relationship between angular distortion and plastic strain

Figure 18 shows the relationship between the final angular distoribution and the number of passes in the transverse direction. The angular distortion is calculated from curvature by assumption that the weld metal of each pass has 4 mm in thickness and 11 mm in width. The full line and the broken line indicate the results by using Material 1 (See **Fig. 2**) having interpass temperature 0°C and 150°C respectively and one dotted chain line the result calculated at interpass temperature 0°C by using Material 2 (See **Fig. 2**). From the above results it is clear that the higher the interpass temperature is, the smaller the final angular distortion becomes with the same weld pass and the higher the yield strength of weld metal is the smaller the final angular distortion becomes.

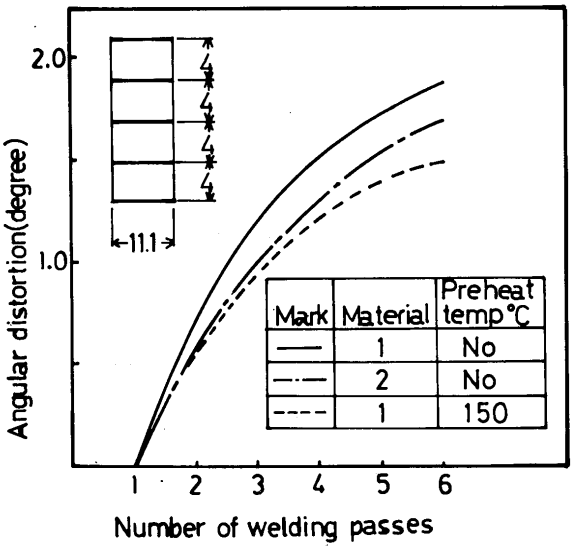

Fig. 18. Effects of interpass temperature and yield strength of weld metal on the angular distortion.

Figure 19 shows the relationship between the final angular distortion and the residual plastic strain produced on the back surface of the first pass under the same conditions as mentioned above. It indicates that plastic strain varies with the conditions although the value of angular distortion is constant.

Recently, Cranfield test has been performed with regard to root crack produced on the heat affected zone of multi-pass welding for high strength steel.[9] It may be considered that the dynamical conditions under which crack is produced in Cranfield test are stress and strain in the vicinity of the root by multi-pass welding. As it is difficult to measure the actual stress and strain in the vicinity of the root, angular distortion until the crack initiation is actually measured as engineering purposes. It should be noted that the relationship between the final angular distortion and plastic strain varies with the conditions as shown in **Fig. 19.**

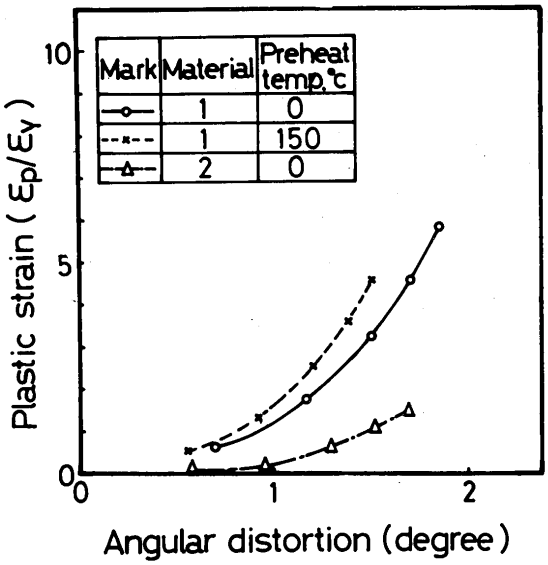

Fig. 19. Relationship between plastic strain on the back surface of the first pass and the angular distortion under several weld conditions.

6. Conclusion

The following conclusions were obtained in this study.

1) The behavior of local thermal stress and strain in

the weld metal during multi-pass welding is clarified by thermal elasto-plastic analysis using a simple one-dimensional model.

2) Residual stress in the transverse direction on the back surface of the first pass is tensile, which corresponds to the yield strength of the average temperature and becomes higher as the number of passes increases. On the front surface of the last pass, compressive residual stress exists in the case of the smaller number of passes, but it transfers towards the tensile side as the number of passes increases. (**Fig. 11 (a)**)
3) A high tensile residual stress exists at the front surface of the pass just below the last pass both in the transverse and longitudinal direction. (**Fig.11**)
4) Existence of residual stress by the preceding weld has little influence on residual stress distribution produced in multi-pass welding. (**Fig. 6**)
5) In the transverse direction, a high tensile plastic strain on the back surface of each pass occurs. (**Fig. 13 (a)**)
6) Residual stress and plastic strain on the back surface by a large heat input welding become smaller than those by a small heat input welding. (**Fig. 15**).
7) The relationship between the final angular distortion and plastic strain on the back surface of the first pass varies with weld conditions. (**Fig. 19**)

Acknowledgment

We whish to express our gratitude for the useful discussions on this study from all the members of Research Committee of Weld Structure of Japan Welding Engineering Society.

References

1) For example, M. Watanabe, K. Satoh; "Welding Dynamics and Its Application" (in Japanese)
2) Y. Ueda; "Analysis of Thermal Elastic-Plastic Stress and Strain during Welding" IIW X-616-71.
3) Y. Fujita, T. Nomoto; "Study on Thermal Elastic-Plastic Problems (Report 1)" Jounal of the society of naval architects of Japan Vol. 130 (1971) (in Japanese)
4) I. Tsuji; "Studies on Elastoplastic Thermal Stresses in Rectangular Plates with Uniaxial Temperature Variation (1st Report)" Journal of the society of naval architects of Japan Vol. 115 (1964) (in Japanese)
5) K. Satoh, S. Matsui; "Reaction stress and weld cracking under Hindered Contraction" IIW IX-574-68
6) T. Kobayashi, K. Nishikawa, H. Tamura; "Reheat Crack at Multi-Pass Weld of High Strength Steel" Preprint of Autumn Meeting of the J.W.S. (1972) (in Japanese)
7) T. Okumura, M. Araki, Y. Noto; "Transverse Crack with Submerged Arc Welding of HT80" Preprint of Spring Meeting of J.W.S. (1972) (in Japanese)
8) M. Araki, Y. Noto, H. Harasawa; "Crack Produced on Multi-Pass Fillet Weld of HT80" Preprint of Spring Meeting of J.W.S. (1972) (in Japanese)
9) For example, M. Ukita, M. Araki, T. Nagao, H. Harasawa; "Crack Produced on Multi-Pass Fillet Weld" Preprint of Autumn Meeting of J.W.S. (1972) (in Japanese)